



## Passive DSSS: Empowering the Downlink Communication for Backscatter Systems

Songfan Li, Hui Zheng, Chong Zhang, Yihang Song, Shen Yang, Minghua Chen,  
and Li Lu, *University of Electronic Science and Technology of China (UESTC)*;  
Mo Li, *Nanyang Technological University (NTU)*

<https://www.usenix.org/conference/nsdi22/presentation/li-songfan>

This paper is included in the Proceedings of the  
19th USENIX Symposium on Networked Systems  
Design and Implementation.

April 4–6, 2022 • Renton, WA, USA

978-1-939133-27-4

Open access to the Proceedings of the  
19th USENIX Symposium on Networked  
Systems Design and Implementation  
is sponsored by



جامعة الملك عبد الله  
للعلوم والتقنية  
King Abdullah University of  
Science and Technology

# Passive DSSS: Empowering the Downlink Communication for Backscatter Systems

Songfan Li<sup>1</sup>, Hui Zheng<sup>1</sup>, Chong Zhang<sup>1</sup>, Yihang Song<sup>1</sup>, Shen Yang<sup>1</sup>, Minghua Chen<sup>1</sup>, Li Lu<sup>1</sup> and Mo Li<sup>2</sup>  
<sup>1</sup>University of Electronic Science and Technology of China (UESTC),  
<sup>2</sup>Nanyang Technological University (NTU)

## Abstract

The uplink and downlink transmissions in most backscatter communication systems are highly asymmetric. The downlink transmission often suffers from its short range and vulnerability to interference, which limits the practical application and deployment of backscatter communication systems. In this paper, we propose *passive DSSS* to improve the downlink communication for practical backscatter systems. Passive DSSS is able to increase the downlink signal-to-interference-plus-noise ratio (SINR) by using direct sequence spread-spectrum (DSSS) techniques to suppress interference and noise. The key challenge lies in the demodulation of DSSS signals, where the conventional solutions require power-hungry computations to synchronize a locally generated spreading code with the received DSSS signal, which is infeasible on energy-constrained backscatter devices. Passive DSSS addresses such a challenge by shifting the generation and synchronization of the spreading code from the receiver to the gateway side, and therefore achieves ultra-low power DSSS demodulation. We prototype passive DSSS for proof of concept. The experimental results show that passive DSSS improves the downlink SINR by 16.5 dB, which translates to a longer effective downlink range for backscatter communication systems.

## 1 Introduction

Passive communication is expected to be a promising connectivity paradigm for building Internet of things (IoT) due to its ultra-low power and low-cost features. Significant efforts have been put into improving the backscatter link of passive communication, in terms of range [43, 49, 53–56], robustness [23, 33, 59], and interoperability with commercial radios like Wi-Fi [25, 26] and LoRa [43, 49]. In particular, unlike RFID that communicates while harvesting RF power, advanced backscatter communication decouples the communication from RF power harvesting [50], and thus becomes a low-power communication solution for IoT devices with longer communication range and limited power supplies (*e.g.*, with small batteries or energy harvesting modules).

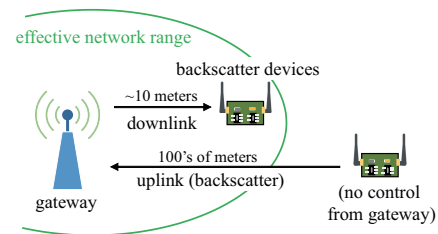


Figure 1: Passive DSSS addresses the asymmetric link issue by empowering the downlink with interference resilience.

Practical deployment of backscatter communication systems faces major challenges in communication asymmetry. As Fig. 1 shows, the backscatter link (uplink) of passive communication and its downlink are often highly asymmetric, where the downlink transmission has poorer performance than the uplink in terms of its range and interference resilience. In most backscatter communication systems, we have a powerful gateway that can be comprehensively designed to demodulate and decode noisy signals on the backscatter uplink. On the downlink, however, receivers on backscatter devices are low power operated and vulnerable to interference and noise.

In practice, IoT devices often need downlink controls. For example, when a communication collision occurs among multiple backscatter devices, the gateway needs to send downlink controls to mediate those devices so as to resolve the collision. Other useful downlink transmissions include scheduling transmissions [15], synchronizing networks [12], sending wake-up packets [22], controlling sensors [28] and implementing over-the-air (OTA) firmware update [61] and so on. The poor communication performance of the downlink becomes a major limit to the range of the backscatter communication system.

In this paper, we ask whether it is possible to significantly improve the downlink resilience to interference. Essentially, for improving the downlink communication, we need to increase the signal quality in terms of signal-to-interference-plus-noise ratio (SINR). Rather than increasing the trans-

mission power of the downlink signal which is essentially limited by radio spectrum regulators like FCC [7] and may lead to undesired extra interference, in this paper we look for a solution that suppresses the interference on the other hand. We make use of spread-spectrum modulation schemes (e.g., DSSS) to suppress interference and noise. However, to the best of our knowledge, none of the existing spread-spectrum schemes can directly work for the downlink of backscatter systems. Specifically, those spread-spectrum systems require the receiver to incorporate a high frequency oscillator to correlate with the received spread-spectrum signal [6], which inevitably incurs high power consumption that is undesirable for energy-constrained backscatter devices.

We present passive DSSS, the first direct sequence spread-spectrum (DSSS) technique for passive communication to suppress interference and noise. As Fig. 2(a) shows, in conventional DSSS communication, the receiver requires complex receiver circuitry and expensive computations for synchronization between the received DSSS signal and locally generated spreading code. Specifically, the DSSS transmitter spreads the frequency spectrum of baseband signals across a wider band by modulation with a pseudorandom spreading code. The DSSS receiver strips off the spreading code and retrieves the original baseband by de-spreading (demodulating) the received signal with a synchronized replica of the spreading code. The de-spreading process requires computationally expensive synchronization between the DSSS signal and local spreading code, which is infeasible on backscatter devices.

To address the challenges associated with the complicated de-spreading of DSSS demodulation, the proposed solution offloads the spreading code generation and synchronization from the backscatter device to the gateway side. As shown in Fig. 2(b), the gateway transmits the DSSS signal and the spreading code reference simultaneously via two separate channels to the receiver. As the spreading code is inherently synchronized with the DSSS signal at the transmitter side, there is no more need for synchronization at the receiver side for de-spreading. The spreading code can be stripped off by combining the two channels together after removing the carrier waves. To achieve passive DSSS in practice, we need to address the following three technical challenges.

*Challenge-1.* Conventional DSSS systems suppose that the receiver can estimate phase information of the channel. However, obtaining phase information needs the use of a local oscillator operating at the carrier frequency, which is infeasible on backscatter devices. In passive DSSS, we leverage the envelope of an RF carrier to convey the DSSS signal (§ 3). Specifically, the gateway transmits the spreading code by modulating the amplitude of the carrier, while the baseband signal is communicated by modulating the phase difference between the synchronized spreading codes in each individual channel. The receiver reconstructs the baseband by comparing the two spreading codes.

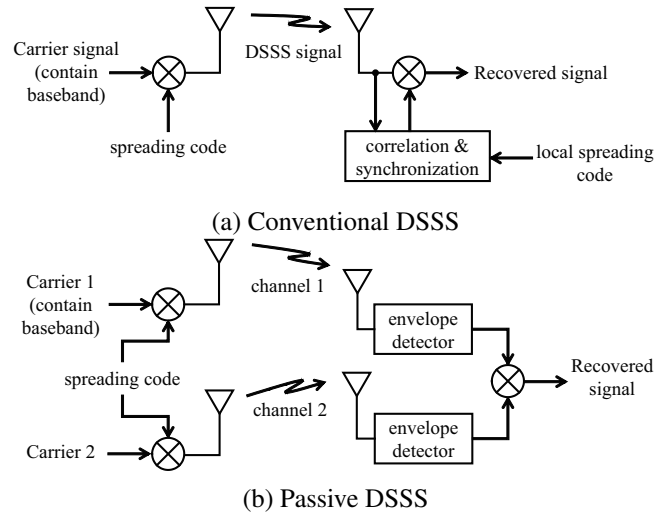


Figure 2: Passive DSSS shifts the synchronization of the spreading code to a gateway, thereby enabling backscatter devices to demodulate DSSS transmission.

*Challenge-2.* The two separate channels to convey the DSSS signal and the spreading code may experience different interference effects in practice. In conventional DSSS receivers, interference is suppressed by multiplying with a spreading code in the de-spreading process. In passive DSSS, however, the de-spreading process performs the multiplication of two channel signals, thus leading to an interference composition (the product of interference signals from two channels). We explore the fact that the interference signals between the separate channels are often independent of each other and propose a solution (§ 4) to suppress the interference composition by calculating the cross-correlation between the two interfered signals.

*Challenge-3.* Conventional correlation operation requires power-consuming digitization and signal processing which cannot be accommodated on backscatter devices. To overcome this challenge, we design an interference cancellation circuit with analog components to compute the cross-correlation (§ 5). As the received signals from two channels are already multiplied with each other in the de-spreading process, the interference cancellation circuit mainly performs the integration of the signal output from the de-spreading process in analog domain. The original baseband signal predominates in the output of the cancellation circuit.

We build a prototype system for proof of concept. We implement the gateway with NI USRP 2922 and implement the passive DSSS receiver with commercial off-the-shelf (COTS) hardware components. The passive DSSS receiver consumes  $166.5 \mu\text{W}$  power when demodulating the DSSS signals robustly with 1 MHz bandwidth. We evaluate the prototype system with realistic communication environments with RFID and LoRa interference. We also conduct stress-testing experiments to examine the performance of passive DSSS in terms

of BER with different noise and interference levels. The results show that passive DSSS can gain an SINR improvement of 16.5 dB over conventional receivers on backscatter devices. The higher SINR translates to a longer effective downlink range for backscatter systems. Our experimental results show that the effective downlink range is extended by up to 52 m with 20 dBm transmission power, which is 3x longer than what can be offered by conventional receivers.

## 2 Preliminary

This section describes the preliminary knowledge before we come to the design of passive DSSS, including descriptions of the reason why DSSS techniques can suppress interference, and the synchronization problem to achieve DSSS on backscatter devices.

### 2.1 A Primer for Conventional DSSS

DSSS is a spread-spectrum modulation technique primarily used for reducing overall signal interference. While DSSS is also employed to achieve concurrent transmissions by the code-division multiple access (CDMA) method in wireless systems (*e.g.*, cellular and GPS), this paper aims to exploit the interference resilience of DSSS to improve the downlink of backscatter communication systems.

Non-spread spectrum wireless communication transmits baseband information by modulating an RF carrier, which can be treated as a narrowband signal that is easily disturbed by any other interferers in the same band. The idea behind spread-spectrum is to use a wider bandwidth than the original baseband (typically 10–60 dB), and therefore diffuses the information across a larger bandwidth, which allows recovery of the transmitted signal even when a part of the spectrum is significantly impaired by narrowband interference.

To achieve DSSS transmission, spread-spectrum modulation is applied on top of conventional modulation by multiplication with the corresponding spreading code before transmission. The spreading code is a pseudorandom sequence with a much higher data rate than the baseband. The produced signal stream thus has a higher data rate and occupies a wider signal bandwidth.

A despreading operation at the receiver side reconstitutes the information in its original bandwidth. The received signal is multiplied by a replica of the spreading code  $\hat{c}(t)$  in order to regenerate the original data. The despreading operation can be mathematically represented as:

$$\begin{aligned}
 & \overbrace{[b(t)c(t) + I(t)]}^{\text{received signal}} \cdot \hat{c}(t) \\
 = & \underbrace{b(t)c(t)\hat{c}(t)}_{\text{despreading}} + \underbrace{I(t)\hat{c}(t)}_{\text{suppression}} \quad (1)
 \end{aligned}$$

where  $b(t)$  is the original baseband signal,  $c(t)$  represents the spreading code, and  $I(t)$  refers to the interference. If  $\hat{c}(t)$  is precisely synchronized with  $c(t)$ , we say  $\hat{c}(t) = c(t)$ . Since  $c(t) = \pm 1$ , the product  $c(t)\hat{c}(t)$  is unity when they are synchronized, so that the first term (despreading) is equal to the desired baseband  $b(t)$ . In the second term (suppression), the interference signal is multiplied by the spreading code, which spreads the interference spectrum. As the spread interference features much higher data rates than the baseband signal, we can remove the interference with a low pass filter (LPF).

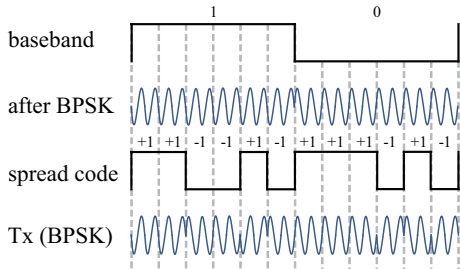
### 2.2 Problem of DSSS Synchronization

If the spreading code is synchronized, the output of a despreading operation will be a correct baseband signal. Otherwise, the received spread-spectrum signal cannot be demodulated correctly because  $c(t)\hat{c}(t)$  will be a noise-like rapidly moving code which hides the baseband signal. It is difficult for a receiver to accurately recover the slow baseband signal without having an exact replica of the spreading code.

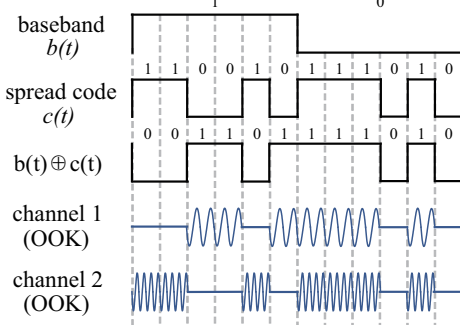
The synchronization process, however, requires that the DSSS receiver performs phase estimation and intensive computation, neither of which is suitable for backscatter devices. Specifically, the synchronization is often accomplished with two steps, *i.e.*, *acquisition* and *tracking*. First, *acquisition* determines the phase of the spreading sequence in the received signal. The *tracking* step then continuously maintains the best alignment between the locally generated spreading code and the received DSSS signal. Although prior works have proposed low-power DSSS techniques [6, 13, 21, 34, 36] to reduce the power consumption for synchronization, they are designed for active radios in which power-starving oscillators and analog-to-digital converters (ADC) are employed in their architectures. Those components typically consume at the scale of *mW*, which is still higher than what can be afforded on backscatter devices.

There are also prior works that apply DSSS in RFID systems. Arthaber *et al.* [2] adopt DSSS to increase the tag-to-reader communication range for RFID, in which each backscatter tag is assigned a unique spreading code to encode the backscatter data. Some works employ CDMA to address the problem of collisions [38, 59, 62] in RFID networks. The code is designed to be orthogonal and thus allows an RFID reader to decode the transmitted data even in presence of collisions. Those works, however, are designed for the uplink transmission from the backscatter tag to the reader, where the power consuming and computationally expensive synchronization process is performed at the reader side.

A recent work  $\mu$ code [41] proposes a CDMA-like method to turbocharge tag-to-tag backscatter communication. Instead of using a pseudorandom spreading code,  $\mu$ code leverages a periodic signal with an alternating one-zero sequence in the transmission to avoid the synchronization at the receiver side. However, the periodic signal is unable to spread the baseband



(a) Conventional DSSS modulation



(b) Passive DSSS modulation

Figure 3: Comparison between conventional DSSS and passive DSSS transmission

signal over a wide frequency band and thus cannot offer the desired anti-interference feature. In conclusion, in order to suppress interference, passive DSSS has to make use of the spreading code in the downlink transmission and address the synchronization problem at the receiver on backscatter devices.

### 3 Passive DSSS Modulation and Transmission

We design a passive DSSS modulation scheme for spread-spectrum signal transmissions without phase estimation on the receiver side. The basic intuition comes from an observation, where receivers on backscatter devices can effectively detect the amplitude information from the incoming signal with simple envelope detection. The envelope detector can be built with passive components such as resistors, capacitors and diodes, and is thus ultra-low power in nature. The designed passive DSSS may utilize the envelope of the carrier signal to convey synchronized spreading codes in two individual channels and leverage the phase difference between the spreading codes to represent the baseband information. Specifically, the gateway conveys an unmodulated spreading code  $c(t)$  via one channel (channel 2 as illustrated in Fig. 3(b)) by modulating the envelope of the RF carrier with on-off keying (OOK) modulation. In the other channel (channel 1), the gateway simultaneously conveys a modulated spreading code  $b(t) \oplus c(t)$  where the baseband modulates the phase of the spreading code. With the above, the passive DSSS receiver can reconsti-

Table 1: XOR operation works as BPSK modulation to the spreading code  $c(t)$ .

	$b(t)$	$c(t)$	$b(t) \oplus c(t)$
no phase change	0	0	0
	0	1	1
$\pi$ phase change	1	0	1
	1	1	0

tute the baseband by comparing the phase shift between the received signals from the two channels.

Figure 3 presents a comparison between the modulation schemes of conventional and passive DSSS. To convey the baseband information by the phase difference, passive DSSS employs an XOR operation to apply the binary phase shift keying (BPSK) modulation to the spreading code. Table 1 shows the truth table of two inputs and their XOR output. We see that when  $b(t) = 0$ , the XOR output has no change to  $c(t)$ , whereas when  $b(t) = 1$  the output is inverted, performing a  $\pi$  phase change to the spreading signal  $c(t)$ . Therefore, the two spreading codes carried in the two channels are  $b(t) \oplus c(t)$  (channel 1) and  $c(t)$  (channel 2) respectively.

At the receiver side, the passive DSSS transmission is demodulated with two steps. First, the spreading code carried in each channel is obtained with envelope detection. Second, the baseband signal can be recovered by despreading, where an XOR gate is employed to perform symmetrical BPSK demodulation by combining the spreading codes from both channels. Since the spreading codes  $b(t) \oplus c(t)$  and  $c(t)$  are synchronized by transmission, the XOR gate derives  $b(t) \oplus c(t) \oplus c(t)$  and retrieves the baseband  $b(t)$ .

## 4 Interference Suppression

We have described the basic idea of passive DSSS. In this section, we discuss the rationale of interference suppression provided by passive DSSS.

### 4.1 Realistic Interference Signals

ISM bands are often approved for license-free which can be used without a government license. This means that multiple types of radio applications may share the same radio spectrum and interfere with each other. This issue increasingly challenges the receivers on backscatter devices because their poor performance cannot provide interference-tolerant downlink communication.

We survey ambient RF signals in 915MHz and 2.4GHz ISM bands in practice at an office and a shopping mall, respectively. In experiments, we use the Keysight N9912A RF handheld analyzer to collect the in-band signals and observe the spectrum of those signals. To quantitatively identify which signals are potential interference, we run two wireless sys-

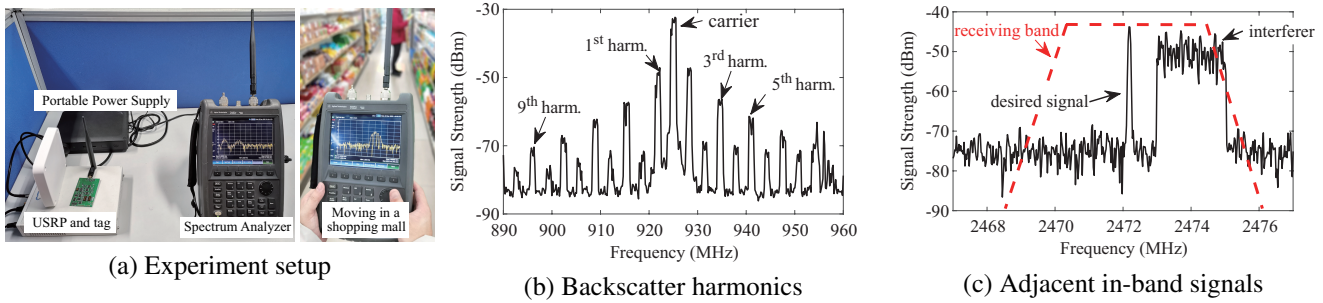


Figure 4: (a) RF interference measurement setup. Typical interference signals (b) and (c) in ISM bands.

tems in our experiments, where one is a 915MHz backscatter system with 1 Mbps chirp modulation, and the other is for 200 kbps downlink ASK transmission to a 2.4GHz backscatter tag. Figure 4(a) presents the experiment setup. With an observation over one week, we summarize three common interference types observed in below.

- *Harmonics*: Backscatter signals are generated by switching the antenna impedance between different loads. The harmonics when backscattering may result in interference in adjacent frequencies, which even spreads over a wide band (Fig. 4(b)). Although prior works exploited solutions including single sideband backscatter [18] and backscatter harmonic cancellation [49] to reduce the harmonic interference, some other backscatter systems may intentionally create stronger harmonics to convey information such as cross frequency communication [1] and localization [35]. Therefore, the harmonics may have a strong presence in ISM bands, leading to disturbance to backscatter networks.
- *Adjacent in-band signals*: The second type of interference is the disturbance from adjacent band signals. Fig. 4(c) presents an example where the backscatter tag receives the adjacent signal within the receiving band, which causes significant interference to the downlink transmission. Although some digital band-pass filtering techniques may be applied to remove the adjacent interference, they are often computationally expensive and thus unfit for backscatter devices.
- *Overlapping signals*: The third case is when two signals overlap in frequency and become interference to each other. Although existing RFID systems provide the frequency hopping mode, it is only available for preventing interference on the uplink in dense reader environments, and cannot resist interference on the downlink.

As a consequence, existing receivers on backscatter devices do not have an effective solution against the realistic interference existing in ISM bands. In the next portion, we illustrate how passive DSSS suppresses the interference in principle.

## 4.2 Interference Suppression in Passive DSSS

We take all of the above interference signals into account. Mathematically, the interference signal is added to the received signal. We denote the received signal with interference at channel 1 by  $S_1(t) + I_1(t)$ , where  $S_1(t)$  represents the DSSS signal envelope transmitted from the gateway, and  $I_1(t)$  is a bipolar interference effect on the signal envelope. If  $I_1(t)$  is a negative value, a bit “1 → 0” error may occur, and vice versa. Similarly, the received signal at channel 2 can be represented as  $S_2(t) + I_2(t)$ .

As illustrated in § 3, the received envelopes from the two separate channels are input into an XOR gate for de-spreading and interference suppression. Such a process can be formulated as:

$$[S_1(t) + I_1(t)] \oplus [S_2(t) + I_2(t)]$$

As XOR operation for binary signals can be derived by  $a \oplus b = a + b - 2ab$ , the above process can be written as:

$$\begin{aligned}
 & \underbrace{S_1(t) + S_2(t) - 2S_1(t) \cdot S_2(t)}_{\text{① despreading}} \\
 & + \underbrace{[1 - 2S_2(t)] \cdot I_1(t) + [1 - 2S_1(t)] \cdot I_2(t)}_{\text{② suppression}} \\
 & - \underbrace{2I_1(t) \cdot I_2(t)}_{\text{③ product of interference}} \tag{2}
 \end{aligned}$$

where the first term ① is equal to  $S_1(t) \oplus S_2(t)$ , thereby performing the de-spreading operation to regenerate the base-band signal.

The second term ② contains the interference signals  $I_1(t)$  and  $I_2(t)$  from the two channels, which however are suppressed by the spreading code from the other channel, respectively. To understand this, we say that  $S_1(t)$  and  $S_2(t)$  are polar envelope signals (between 0 and 1) that comprise the spreading code, while  $I_1(t)$  and  $I_2(t)$  are bipolar signals (between -1 and +1) representing the possible information disturbance (bit 1 → 0 or bit 0 → 1). Therefore, the term  $1 - 2S_1(t)$  is equivalent to converting  $S_1(t)$  to a bipolar signal and inverting its polarity, which does not change the spreading code in terms of data rate. Hence, the interference effects in

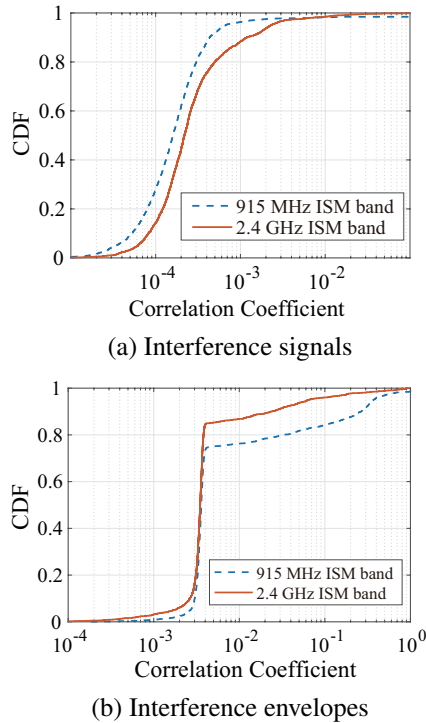


Figure 5: (a) The correlation of the interference signals from two individual channels. (b) The correlation of their envelopes.

the second term are suppressed by the multiplication with the bipolar spreading code.

However, the third term ③ does not contain the spreading code. The product of the two interference compositions is still an interference signal to baseband. To mitigate the interference, existing solutions can be categorized into the following three types. First, the receiver may divide the received signal bandwidth into multiple sub-bands, and then position sub-band notch filters (band-stop) to suppress the interferer [8, 9, 42]. Second, statistical methods may be used at the receiver to average the interference signal over multiple symbols [63]. Third, feedback loop mechanisms may be used to enhance the desired signal by iterative correlation [10], in which each loop iteration makes the desired signal cleaner. All of the above methods, however, require power-starving digital signal processing [37] which is not suitable for backscatter devices.

Fortunately, we observe that the two interference signals in each individual channel are almost independent of each other. To verify this, we conduct a one-week measurement in real environments. In 915 MHz ISM band, we turn on the backscatter tag in Fig. 4(b) to emulate interference from backscatter networks. In 2.4 GHz ISM band, we choose an in-door environment where two Wi-Fi routers and a number of Bluetooth devices operate. At least ten Wi-Fi channels and sixteen Bluetooth channels have strong signal presence.

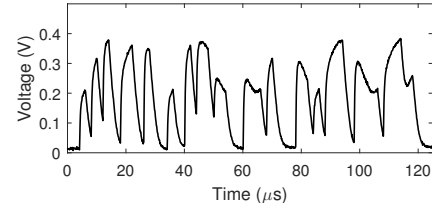


Figure 6: The signal envelope distorted by interference is full analog.

We employ a USRP to arbitrarily pick two separate channels with 1 MHz bandwidth in the ISM bands respectively, and compute the correlation between the interference signals over the two channels. Figure 5 plots the results of the correlation between the two interference signals and their envelopes. If an interference signal resembles the other one, the correlation coefficient will be close to 1. We see that the overall correlation remains statistically very low, indicating almost uncorrelated interference signals.

Given the low interference correlation, we can cancel the interference signals after the de-spreading by computing the correlation of the two interference compositions in the third term, given by:

$$\int_0^T I_1(t) \cdot I_2(t) dt \approx 0 \quad (3)$$

where  $T$  is the duration of the de-spreading process that provides the calculation of the dot product operation. In section § 6.4.2, we evaluate the performance of passive DSSS over the interference of different correlation coefficients.

## 5 Low Power DSSS De-spreading

In this section, we present the hardware design to implement the design rationale described in 4.2. At a high level, the passive DSSS receiver first obtains the envelopes of the spread-spectrum signals and inputs the envelope waveforms into an XOR gate for despreading. The receiver further employs a hybrid analog-digital computing circuit to derive the signal correlation in order to suppress the interference.

### 5.1 Despreading Process

We combine the two envelope signals with an XOR gate to perform the despreading process. However, when the transmission is disturbed by interference in the wireless channels, the signal envelope captured from the air is fully analog as shown in Fig. 6. The XOR gate is a digital component and thus only accepts digital signal inputs, meaning that the passive DSSS receiver has to digitize the envelope signals before the despreading process. Conventional DSSS receivers in active radios realize digitization with two steps — sampling the

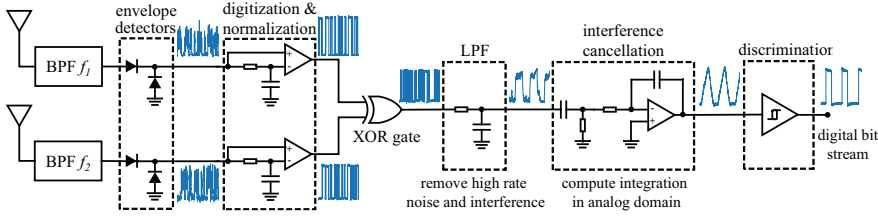


Figure 7: Passive DSSS receiver hardware design.

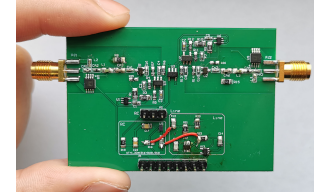


Figure 8: Passive DSSS receiver prototype.

voltage signal with a precise ADC (*e.g.*, 8-12 bit) and then discriminating the binary value according to a decision-making criterion (*e.g.*, maximum likelihood estimation). The two steps involved in active radios are not feasible on backscatter devices due to the high power consumption. Additionally, due to frequency selective fading on the two separate channels, the received envelope signals may experience different amplitude attenuation, meaning that the two-channel signals should not be directly combined without normalization.

Passive DSSS receivers adopt an ultra-low power digitization method, where a one-bit ADC (*i.e.*, comparator) is used instead of a high precision ADC to threshold the analog envelope signals, and discriminate the digital value by its moving average. Specifically, the comparator compares the analog envelope voltage and the moving average of the envelope in order to distinguish between the two binary levels at the output of the envelope detector. The moving average is automatically computed by an RC low-pass circuit at one input of the comparator, and thus creates a dynamic threshold for digitizing different input signal amplitudes. In addition, the one-bit ADC also normalizes the received signal from each channel, so the output of digitization can be directly supplied to the XOR gate for DSSS despreading.

Figure 7 gives the hardware design of the passive DSSS receiver. The two receiver branches are designed symmetrically in order to maintain the synchronization of the received spread-spectrum signals between the two channels. The bandpass filters (BPF) are employed to achieve frequency band selection that isolates the signal from the other channel. The envelope detector then removes the carrier waves of the incoming signals in both channels and outputs the envelope waveforms. Further, the one-bit digitization circuit digitizes the disturbed envelopes and sends them into the XOR gate for the despreading process.

## 5.2 Analog-Digital Correlation Computation

Another problem to achieve the passive DSSS receiver is that computing correlation involves intensive computations [14] that are unacceptable to backscatter devices. To address this, we design a hybrid analog-digital computing circuit (see Fig. 7) to compute the correlation for interference suppression with ultra-low power. At a high level, the XOR gate performs a digital operation which comprises the multiplication of the

two interference signals (Eq. 2, the third term). Therefore, we further design an analog interference cancellation circuit to compute the integration of the XOR output to suppress the interference composition in analog domain.

To understand our design, we recall the despreading process described in § 4.2. The despreading result at the output of the XOR gate includes three basic compositions: the desired baseband, the suppressed interference and the product of the two interference signals. We first remove the suppressed interference using an RC-based LPF because they contain the spreading codes that have much higher data rates (frequencies) than the baseband. Then, the interference cancellation circuit performs an integration operation over the rest of the signals in order to remove the interference product composition. The interference cancellation process can be represented as:

$$\begin{aligned}
 & \int_0^T [S_1(t) \oplus S_2(t)] - 2[I_1(t) \cdot I_2(t)] dt \\
 &= \int_0^T b(t) dt - 2 \int_0^T I_1(t) \cdot I_2(t) dt \\
 &\approx \int_0^T b(t) dt
 \end{aligned}$$

According to Eq. 3, the product integration of the interference signals is negligible due to their low correlation. Therefore, the result of the interference cancellation is approximately equal to the integration of the baseband signal. Further, as the baseband comprises ones and zeros that are represented by logical high and low voltages, we can discriminate the baseband data according to the energy difference between ones and zeros. Finally, the discrimination output is a digital bit stream representing the baseband data and can be directly handled by the MCU of the device.

The interference cancellation circuit incorporates a DC block capacitor and an analog linear integrator. The DC block capacitor precedes the integrator in order to convert the polarity of the output signals of LPF from polar to bipolar. The bipolar signals facilitate the subsequent integrator in performing integration.

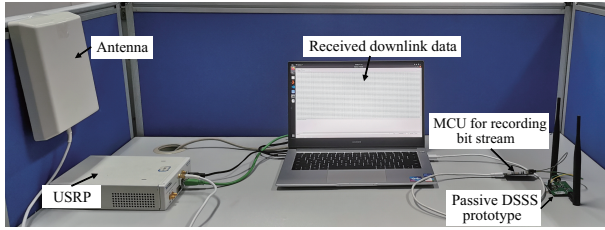


Figure 9: Experimental setup.

## 6 Evaluation

We describe the implementation experience of the passive DSSS prototype in § 6.1 and discuss its power consumption. In § 6.2, we evaluate the communication performance of passive DSSS and decide the baseline for subsequent evaluations. Further, we evaluate passive DSSS with the interference from real world environments and also estimate the communication range of passive DSSS in § 6.3. We evaluate the performance boundary of passive DSSS with stress-test in § 6.4. Finally, we discuss the application case study in § 6.5.

### 6.1 Implementation

We implement our passive DSSS receiver prototype (Fig. 8) with commercial off-the-shelf (COTS) components. We employ the SAW BPF filters from NMRF (one is 890 MHz~915 MHz, the other is 920 MHz~925 MHz) to distinguish between the two channels. The envelope detectors adopt the Schottky diodes HSMS-285C. As the filters and diodes are passive components, they do not consume power. Further, the 1-bit digitization circuit is built with the NCS2200 comparator. The pair of digitization circuits consume 20  $\mu$ A current. Next, the XOR gate is implemented using SN74LV1T86 from Texas Instruments (1.25  $\mu$ A current consumption), and the cutoff frequency of the RC-based LPF is set to twice the baseband frequency. Moreover, the interference cancellation circuit employs a 10 nF DC block capacitor and comprises a power-efficient TSV6390 operational amplifier in the integrator circuit (50  $\mu$ A current consumption). Finally, we use the nano-power comparator MAX40000 (12  $\mu$ A) made by Maxim Integrated for the final discrimination. The output of the discriminator is a digital bit stream that can be directly channeled to an MCU. Since the MCU does not participate in the demodulation process of passive DSSS, we do not consider MCU’s power consumption. According to our measurement study, the passive DSSS receiver totally consumes 166.5  $\mu$ W power when operating with 1 MHz signal bandwidth and 2 V supply voltage. When commercially adopted, the power consumption can be further reduced by application-specific integrated circuit (ASIC) implementation [26, 39, 60].

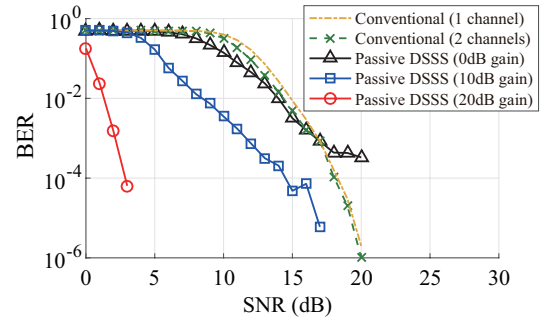


Figure 10: Performance comparison. We choose the case of conventional (2 channels) as the baseline.

### 6.2 Performance and Baseline

Figure 9 depicts the experiment setting where we employ a USRP to send downlink transmissions to our prototype. The received data stream is forwarded by the onboard MCU to the laptop for bit error rate (BER) analysis. While passive DSSS theoretically supports arbitrary digital coding schemes of the baseband, we adopt pulse-interval encoding (PIE) in the experiments for its wide adoption in many passive radios like RFID. To evaluate BER, the USRP transmits one million test bits on the downlink during each time of the measurement to derive the average.

We evaluate the communication performance in terms of BER with noise. Passive DSSS makes use of two channels, whereas conventional receivers on backscatter devices only use one channel for the downlink transmission. In our experiments, we consider both conventional receivers and passive DSSS receivers. We note that the passive DSSS receiver has two symmetric antenna branches, in which each branch is a conventional receiver. Thus, we can employ each antenna branch of the passive DSSS receiver to act as a conventional receiver that shares the same hardware and layout with passive DSSS. The difference is that the conventional receivers receive non-DSSS signals from the gateway. Both receivers used in the experiments utilize the same 500 kHz signal bandwidth. In the evaluation, we use additive white Gaussian noise (AWGN) to adjust SNR of the transmitted signals from the USRP. The noise signals are applied across the entire signal bandwidth.

Figure 10 plots the achieved BER of the conventional and passive DSSS receivers. First, the conventional (1 channel) case gives the measured result when we only use one of the two receiving branches (we obtain the data from one of the inputs of the XOR gate, see Fig. 7). Then, the conventional (2 channels) case gives the results when both two receiving channels are used for the conventional receiver, in which the gateway transmits continuous waves (CW) on the other channel so we can use the same circuit of passive DSSS to demodulate the data. We observe that there is no obvious

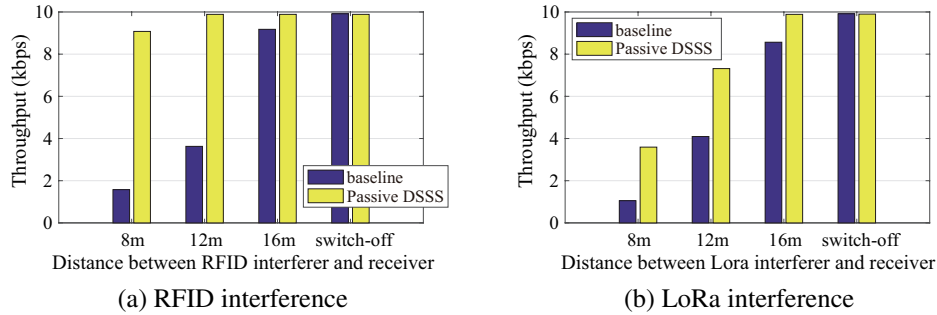


Figure 11: The measured backscatter downlink throughput achieved when RFID or LoRa interference exists. “switch-off” means no interference. We adopt the 20 dB gain for passive DSSS.

BER difference between the single channel and dual channel cases for the conventional receiver.

For passive DSSS, we first see the result of passive DSSS with the 0 dB processing gain, which uses the two receiving channels but no spread-spectrum. The processing gain refers to the ratio of the spread bandwidth to the baseband bandwidth (*i.e.*, 0 dB represents the ratio is 1). Although the performance of passive DSSS (0 dB) has a slight improvement when SNR is below 15 dB, its BER can be higher than the conventional cases especially when SNR is high. This is mainly due to the signal mismatch between the two channels. Specifically, the expectation of ideally synchronized two channels is impractical due to propagation delay on the RF chain of each receiving channel. Next, we maintain the bandwidth and increase the processing gain to 10 dB. We can see that the BER performance is significantly improved. Finally, we also show the BER result of passive DSSS when the gain is increased to 20 dB. As we expected, the higher processing gain leads to improved BER performance because a higher gain can distribute noise into a wider band during the despreading process, thus resulting in a lower noise power spectral density (PSD).

Moreover, we define the effective communication SNR which is the SNR condition that can suppress the BER to below the threshold of  $10^{-2}$ . With 10 dB processing gain passive DSSS is able to obtain an effective SNR improvement of 6 dB, and with 20 dB processing gain it can obtain 12.8 dB improvement. The primary cost is due to the inadequate performance of the simple envelope detector which is inherently prone to noise. Nevertheless, passive DSSS improves on top of the limits of the conventional receivers, and shows better and more controllable performance with the same coarse envelope detector.

In our following evaluation, we choose to use the conventional (2 channels) setting as the *baseline* to demonstrate the comparative advantage of passive DSSS.

## 6.3 Real World Evaluation

### 6.3.1 Realistic Interference Signals

We evaluate the communication performance of passive DSSS with realistic interference from real world. We consider the interference signals from RFID and LoRa transmissions. We employ RFID reader Impinj R420 and LoRa transceiver E32-915T30S from EBYTE as interference sources in the experiment, both of which are configured with 30dBm Tx power. Further, we configure the USRP to transmit downlink data to the receivers, where the passive DSSS transmission has a 20 dB processing gain. We fix the distance between the USRP and receivers at 4 m and vary the distance of the interference source (RFID reader or LoRa transceiver) from 8 to 16 meters away from the receivers. Finally, we switch off the interference source and measure the downlink throughput as a reference.

Figure 11 shows the downlink throughput measurement results under the RFID and LoRa interference. Compared with the baseline approach, passive DSSS can effectively improve the throughput with both RFID and LoRa interference. Further, we can see that passive DSSS can better suppress the interference from RFID than LoRa, mainly because DSSS is inherently suitable for suppressing narrowband interference as the spreading code can distribute the power of the interference signal to a wider band. The RFID interference signals (typical spreading over 100 kHz) are narrower than those from LoRa (250–500 kHz).

### 6.3.2 Communication Range

We evaluate the communication range of the passive DSSS receivers in both line-of-sight (LOS) and non-LOS (NLOS) scenarios. In the experiments, we employ a low-power amplifier TLV9001 after the envelope detection to achieve a lower receiving threshold for weaker signal cases. The amplifier does not increase the SINR of the received signals as it also amplifies noise and interference.

Figure 12 plots the experimental results with LOS. The LOS experiment considers an outdoor street and the USRP

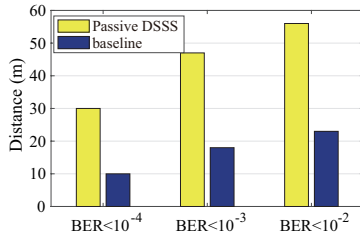
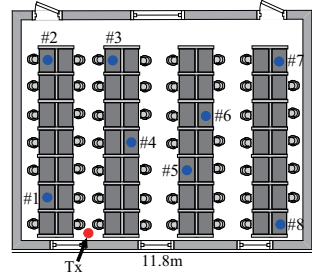
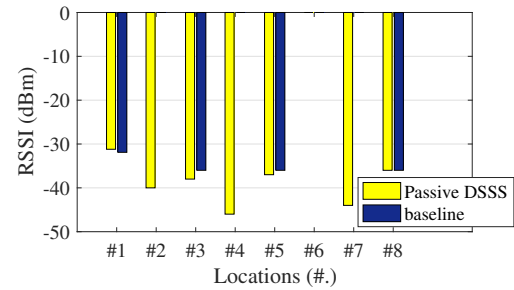


Figure 12: LOS communication range.



(a) NLOS experiment locations



(b) Measured RSS when the BER is below  $10^{-2}$

Figure 13: NLOS communication range.

conveys test bits to the receiver prototypes with 20 dBm transmission power per channel. We incrementally move the receivers away from the USRP transmitter with 1m step length. At each distance, we record the bits received by each receiver to derive the BER. According to different BER thresholds, we can identify three levels of the effective communication range, *i.e.*, excellent ( $BER < 10^{-4}$ ), good ( $BER < 10^{-3}$ ) and fair ( $BER < 10^{-2}$ ). The figure demonstrates that passive DSSS generally extends the communication range by  $\sim 2-3x$  when compared with the baseline. In particular, the gain is 3x for those communications at the level of “excellent”. This is reasonable because passive DSSS uses a wider band to convey the baseband, thus suffering from less noise and interference effects in real environments.

Figure 13 plots the results from the NLOS experiment, where we conduct the experiment in an indoor office. We fix the gateway with 20 dBm transmission power and vary the receivers across 8 different locations within the space as shown in Fig. 13(a). At each location, we measure the BER of the received data for all of the receivers. If the BER is below  $10^{-2}$ , we measure the received signal power (RSS) at the location. We see that passive DSSS works with more locations than the baseline, and discuss the results as follows:

- At locations #2, #4 and #7, only passive DSSS can work. Passive DSSS receiver works with transmissions of RSS as low as -46 dBm owing to its anti-noise capability, while the baseline can only work when the RSS is higher than -36 dBm. As a result, passive DSSS works for nearly all measured locations while the baseline cannot work for half of these locations.
- At location #6, neither passive DSSS nor baseline can work. This location suffers from significant deep fading due to multi-path destructive interference, where both passive DSSS and the baseline do not work.

## 6.4 Stress-test

To evaluate the performance boundary of passive DSSS, we perform stress-tests with the prototype by manually imposing

interference and noise to the channels until the communication corrupts. We employ a USRP as the source of interference.

### 6.4.1 Anti-Interference

In this section we evaluate the performance under interference of different modulated signals. We consider RFID signals as an example of amplitude modulation, LoRa signals as frequency modulation and Wi-Fi signals as phase modulation<sup>1</sup>. To this goal, we employ the USRP to measure real transmissions from the above systems correspondingly and replay the measured signals to interfere with passive DSSS (20 dB processing gain). Figure 14 shows the measured BER of passive DSSS with the presence of the three interference signals, respectively. We have the following three observations:

- Although the rationale of envelope detection is based on the amplitudes of the signal envelopes, various types of interference signals may lead to bit errors, because the carriers have different phases compared to the downlink transmission. As a result, although LoRa and Wi-Fi are not based on amplitude modulation, the received downlink transmission envelopes are still destructed when interfered by those signals due to destructive superposition of the signal phases.
- The conventional receiver is more prone to the interference of the RFID and LoRa transmissions than the Wi-Fi transmissions because those are narrowband interference signals (RFID over 100 kHz and LoRa over 250–500 kHz) which have higher PSD. In contrast, the Wi-Fi interference has lower PSD due to the wider transmission bandwidth (22 MHz) and its use of data whitening to distribute the power evenly within the band.
- LoRa transmissions lead to the strongest interference. We observe that RFID adopts amplitude modulation with PIE encoding, and its interference is weak during the

<sup>1</sup>We switch the setting to the 2.4GHz band for testing the interference from Wi-Fi signals.

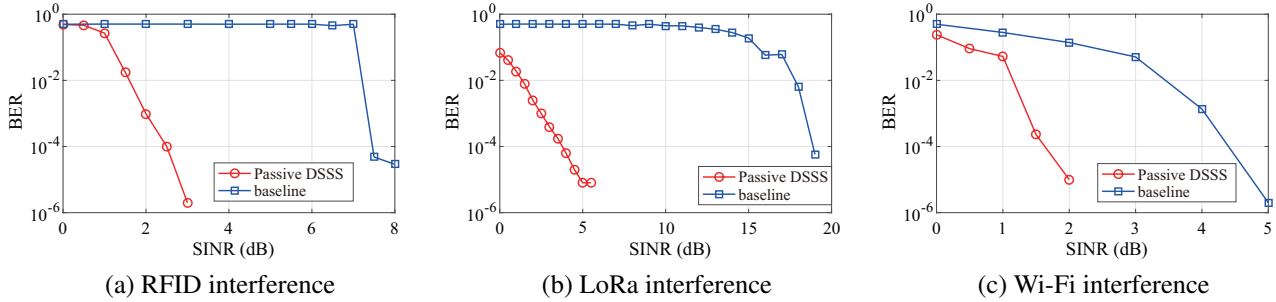


Figure 14: Stress test of interference from RFID, LoRa and Wi-Fi signals.

logic low in PIE symbols. LoRa signals use frequency modulation which does not vary its amplitude, and leads to persistent interference.

In general, compared with the baseline, passive DSSS provides  $\sim 5$ dB,  $\sim 13$ -15dB, and  $\sim 3$ dB gain for RFID, LoRa, and Wi-Fi interference, respectively.

#### 6.4.2 Interference Correlation

We evaluate the performance of passive DSSS with interference of different correlation coefficients between its two communication channels. In the evaluation, we add the same interference signal to both channels and apply AWGN to vary the correlation coefficient between the two channels. Due to the high anti-interference performance, the passive DSSS BER is negligibly low when the SINR is above 3 dB (see Fig. 14). We thus conduct the experiment with transmissions of SINR = 3 dB and examine how the BERs vary when the correlation coefficient across the two channels increases. Figure 15 plots the measured BER of passive DSSS with the RFID, LoRa and Wi-Fi interference. We see that the BER increases when the interference signals on the two channels are more correlated, which is as expected because the despreading quality of passive DSSS depends on the analog integrator to remove the product of the interference compositions on the two channels (Eq. 3). The performance degrades more significantly with the RFID interference than LoRa and Wi-Fi because the ASK signals may directly destruct the envelope of passive DSSS transmissions in both channels.

### 6.5 Case Study

In this section, we demonstrate the benefit of passive DSSS to practical deployment of backscatter systems in a case study with two different types of deployment.

**Monostatic** deployment involves a backscatter gateway that comprises the collocated Tx and Rx (Fig. 16(a)), where the gateway transmits to the backscatter device on the downlink and receives the backscattered transmissions on the uplink. In such a case, the key constraint is that the downlink range limits the coverage of the system. Passive DSSS can

effectively improve the downlink range and increase the coverage. To test this, we incorporate a backscatter uplink with 1 kbps chirp modulation. When using the conventional receiver, the coverage of the backscatter system is limited to the downlink range of 26 m. Passive DSSS improves the coverage to 52 m. We observe that the uplink experiences good performance within the extended coverage. The current gateway Rx sensitivity is  $-97$  dBm, which can be further improved to below  $-130$  dBm [15, 24, 49], which suggests more room of improvement with further extended downlink range.

**Bistatic/Multistatic** deployment is used for long range backscatter communication, where the Tx and Rx gateways are separated (Fig. 16(b)). In practice, multiple Tx gateways are often needed to interrogate the geographically distributed backscatter devices. The short downlink range leads to small coverage of each Tx gateway and as a result more Tx gateways to cover the deployment area. The increased number of gateways may further incur coordination problems among those gateways and lead to higher deployment costs. Passive DSSS mitigates the problem by improving the downlink range. In our experiment, passive DSSS receivers enable the Tx gateway to achieve 4x the coverage area than using the conventional receivers. The uplink distance can arrive at  $\sim 108$  m when the backscatter devices are located at the edge of the downlink range.

## 7 Discussion

**Bandwidth Usage.** As passive DSSS needs two individual channels to transmit the DSSS signals, the bandwidth usage is doubled. Such an issue however is not significant since the downlink to the backscatter devices is typically for control purpose and thus the required bandwidth is small. Our prototype uses 500 kHz for each channel, which is comparable to the bandwidth usage of other IoT communication techniques like LoRa. In addition to that, the gateway can dynamically adjust the bandwidth usage by varying the processing gain in passive DSSS, *e.g.*, the gateway may increase the processing gain to improve interference resilience when detecting interference signals, or reduce the gain for saving the bandwidth usage when the downlink experiences low interference.

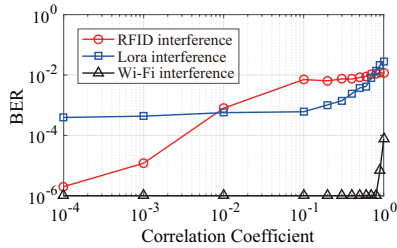


Figure 15: Measured BER with different correlation coefficients between the two passive DSSS channels (SINR=3dB).

**Support for Concurrent Transmissions.** While some uses of DSSS achieve concurrent transmissions with the CDMA method, the current passive DSSS design does not support concurrent transmissions because the spreading code is entirely generated by the gateway, which means that all the receivers share the same spreading code. As passive DSSS only requires small bandwidth for each receiving channel, future research may consider exploring frequency multiplexing schemes like frequency-hopping spread spectrum (FHSS) or frequency division multiple access (FDMA) to support concurrent transmissions for passive DSSS.

**Signal Jamming.** We expect the proposed passive DSSS to make the downlink of backscatter systems resilient to realistic RF interference in practical IoT scenarios. As being discussed in § 4, the interference signals in the two channels are independent and can thus be suppressed by computing the interference correlation. However, if the interference comes from an intentional jamming source, where malicious attackers send a pair of highly correlated interference signals into the two channels, passive DSSS may be compromised. Similarly, high-power interference may impair the SINR over the entire frequency band and thus throttle the communications. We leave the countermeasures to such malicious attacks to future works.

## 8 Related Work

**Passive Radio.** There are tremendous existing works which study the backscatter uplink of passive radios including the research on improving the backscatter data rate [51, 52], throughput [16, 19, 20, 65–67], range [43, 49, 53, 54, 56, 65], robustness [33, 59]. Another compelling direction of research explores the inter-operation between backscatter communication and existing wireless systems such as Wi-Fi [4, 18, 25, 26, 64, 68], BLE [11, 18], Zigbee [29, 44], LoRa [40, 43, 49], FM [57] and LTE [5].

On the other hand, there are also a few works to explore other out-of-band wireless channels to convey downlink data to backscatter devices, including the use of the presence and absence of Wi-Fi packets [25], the lengths of Wi-Fi transmis-

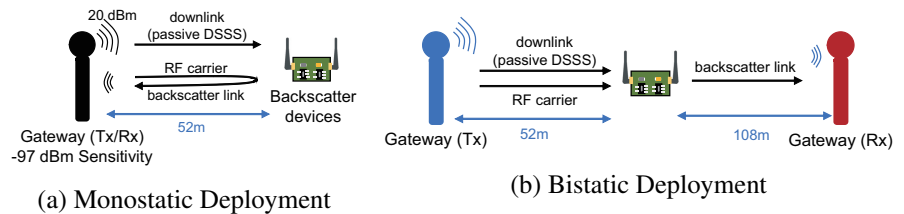


Figure 16: Application case study for passive DSSS.

sions [64], reverse engineering of OFDM [18], perturbations to ambient signals [22], and backscatter signals from other tags [31, 32, 41]. In this paper, the proposed passive DSSS presents a direct in-band solution to the downlink problem and is able to support general backscatter communication systems.

**Functionality Offloading.** The essential idea of backscatter communication is one type of offloading techniques which saves the power consuming RF oscillator in the uplink communication. Recently, a series of works have made great efforts to shift power-starving functionalities from backscatter devices to the gateway side, including storage [48], computation [67], digitization [39, 45], subcarrier generation [47] and sensor control [28]. Passive DSSS by nature belongs to such functionality offloading efforts and shifts the spread-spectrum synchronization to the gateway.

## 9 Conclusion

This paper proposes passive DSSS to empower downlink transmissions with interference and noise resilience for backscatter communication systems. The proposed design exploits interference suppression across two separate wireless channels to achieve ultra-low power demodulation of spectrum spreading signals. The experimental evaluation with real world interference demonstrates the effectiveness of passive DSSS. We envision that the design of passive DSSS opens a door to making passive communication more practical to future wide area IoT systems and applications.

## Acknowledgments

We sincerely thank our shepherd Wenjun Hu and the anonymous reviewers for their helpful feedback in improving this paper. We also thank Jian Li from SICE UESTC for his support for the experiment in Fig. 4(a). This work is supported by the National Natural Science Foundation of China under Grant Nos. U21A20462 and 61872061, and by the Singapore MOE AcRF Tier 2 Grant MOE-T2EP20220-0004.

## References

- [1] Zhenlin An, Qiongzhen Lin, and Lei Yang. Cross-frequency communication: Near-field identification of uhf rfids with wifi! In *Proceedings of the 24th Annual International Conference on Mobile Computing and Networking, MobiCom '18*, pages 623–638, New York, NY, USA, 2018. Association for Computing Machinery.
- [2] Holger Arthaber, Thomas Faseth, and Florian Galler. Spread-spectrum based ranging of passive uhf epc rfid tags. *IEEE Communications Letters*, 19(10):1734–1737, 2015.
- [3] Venkat Arun and Hari Balakrishnan. Rfocus: Beamforming using thousands of passive antennas. In *17th USENIX Symposium on Networked Systems Design and Implementation (NSDI 20)*, pages 1047–1061, Santa Clara, CA, February 2020. USENIX Association.
- [4] Dinesh Bharadia, Kiran Raj Joshi, Manikanta Kotaru, and Sachin Katti. Backfi: High throughput wifi backscatter. In *Proceedings of the 2015 ACM Conference on Special Interest Group on Data Communication, SIGCOMM '15*, pages 283–296, New York, NY, USA, 2015. ACM.
- [5] Zicheng Chi, Xin Liu, Wei Wang, Yao Yao, and Ting Zhu. Leveraging ambient lte traffic for ubiquitous passive communication. In *Proceedings of the Annual conference of the ACM Special Interest Group on Data Communication on the applications, technologies, architectures, and protocols for computer communication*, pages 172–185, 2020.
- [6] Charles Chien, Igor Elgorriaga, and Charles McConaghy. Low-power direct-sequence spread-spectrum modem architecture for distributed wireless sensor networks. In *ISLPED'01: Proceedings of the 2001 International Symposium on Low Power Electronics and Design (IEEE Cat. No. 01TH8581)*, pages 251–254. IEEE, 2001.
- [7] Federal Communications Commission. Regulatory status for using rfid in the epc gen2 (860 to 960 mhz) band of the uhf spectrum. [https://www.gsl.org/docs/epc/uhf\\_regulations.pdf](https://www.gsl.org/docs/epc/uhf_regulations.pdf), 2021.
- [8] S. Cui, K. C. Teh, K. H. Li, Y. L. Guan, and C. L. Law. Narrowband interference suppression in transmitted reference uwb systems with inter-pulse interference. In *2007 IEEE International Conference on Ultra-Wideband*, pages 895–898, 2007.
- [9] Shan Cui, Kah Chan Teh, Kwok H Li, Yong Liang Guan, and Choi Look Law. Performance analysis of transmitted-reference uwb systems with narrowband interference suppression. *Wireless Communications and Mobile Computing*, 9(8):1081–1088, 2009.
- [10] F. Dowla, F. Nekoogar, and A. Spiridon. Interference mitigation in transmitted-reference ultra-wideband (uwb) receivers. In *IEEE Antennas and Propagation Society Symposium, 2004.*, volume 2, pages 1307–1310 Vol.2, 2004.
- [11] Joshua F Ensworth and Matthew S Reynolds. Every smart phone is a backscatter reader: Modulated backscatter compatibility with bluetooth 4.0 low energy (ble) devices. In *2015 IEEE International Conference on RFID (RFID)*, pages 78–85, April 2015.
- [12] Kai Geissdoerfer and Marco Zimmerling. Bootstrapping battery-free wireless networks: Efficient neighbor discovery and synchronization in the face of intermittency. In *18th USENIX Symposium on Networked Systems Design and Implementation (NSDI 21)*, pages 439–455. USENIX Association, April 2021.
- [13] Jafar Ghaisari and Arash Ferdosi. A direct sequence spread spectrum code acquisition circuit for wireless sensor networks. *International Journal of Electronics*, 98(6):793–800, 2011.
- [14] Shyamnath Gollakota, Fadel Adib, Dina Katabi, and Srinivasan Seshan. Clearing the rf smog: Making 802.11n robust to cross-technology interference. In *Proceedings of the ACM SIGCOMM 2011 Conference, SIGCOMM'11*, pages 170–181, New York, NY, USA, 2011. Association for Computing Machinery.
- [15] Mehrdad Hesar, Ali Najafi, and Shyamnath Gollakota. Netscatter: Enabling large-scale backscatter networks. In *Proceedings of the 16th USENIX Conference on Networked Systems Design and Implementation, NSDI'19*, pages 271–283, USA, 2019. USENIX Association.
- [16] Pan Hu, Pengyu Zhang, and Deepak Ganesan. Laissez-faire: Fully asymmetric backscatter communication. In *Proceedings of the 2015 ACM Conference on Special Interest Group on Data Communication, SIGCOMM '15*, pages 255–267, New York, NY, USA, 2015. ACM.
- [17] Pan Hu, Pengyu Zhang, Mohammad Rostami, and Deepak Ganesan. Braidio: An integrated active-passive radio for mobile devices with asymmetric energy budgets. In *Proceedings of the 2016 ACM SIGCOMM Conference, SIGCOMM'16*, pages 384–397, New York, NY, USA, 2016. Association for Computing Machinery.
- [18] Vikram Iyer, Vamsi Talla, Bryce Kellogg, Shyamnath Gollakota, and Joshua Smith. Inter-technology backscatter: Towards internet connectivity for implanted devices. In *Proceedings of the 2016 ACM SIGCOMM Conference, SIGCOMM'16*, pages 356–369, New York, NY, USA, 2016. Association for Computing Machinery.

- [19] Meng Jin, Yuan He, Xin Meng, Dingyi Fang, and Xiaojiang Chen. Parallel backscatter in the wild: When burstiness and randomness play with you. In *Proceedings of the 24th Annual International Conference on Mobile Computing and Networking*, pages 471–485, 2018.
- [20] Meng Jin, Yuan He, Xin Meng, Yilun Zheng, Dingyi Fang, and Xiaojiang Chen. Fliptracer: Practical parallel decoding for backscatter communication. *IEEE/ACM Transactions on Networking*, 27(1):330–343, 2019.
- [21] Inyup Kang and Alan N Willson. Low-power viterbi decoder for cdma mobile terminals. *IEEE journal of solid-state circuits*, 33(3):473–482, 1998.
- [22] Zerina Kapetanovic, Ali Saffari, Ranveer Chandra, and Joshua R. Smith. Glaze: Overlaying occupied spectrum with downlink iot transmissions. *Proc. ACM Interact. Mob. Wearable Ubiquitous Technol.*, 3(4), December 2019.
- [23] Mohamad Katanbaf, Vivek Jain, and Joshua R. Smith. Relacks: Reliable backscatter communication in indoor environments. *Proc. ACM Interact. Mob. Wearable Ubiquitous Technol.*, 4(2), June 2020.
- [24] Mohamad Katanbaf, Anthony Weinand, and Vamsi Talla. Simplifying backscatter deployment: Full-duplex lora backscatter. In *18th USENIX Symposium on Networked Systems Design and Implementation (NSDI 21)*, pages 955–972. USENIX Association, April 2021.
- [25] Bryce Kellogg, Aaron Parks, Shyamnath Gollakota, Joshua R. Smith, and David Wetherall. Wi-fi backscatter: Internet connectivity for rf-powered devices. In *Proceedings of the 2014 ACM Conference on SIGCOMM, SIGCOMM '14*, pages 607–618, New York, NY, USA, 2014. Association for Computing Machinery.
- [26] Bryce Kellogg, Vamsi Talla, Shyamnath Gollakota, and Joshua R. Smith. Passive wi-fi: Bringing low power to wi-fi transmissions. In *Proceedings of the 13th Usenix Conference on Networked Systems Design and Implementation, NSDI'16*, pages 151–164, USA, 2016. USENIX Association.
- [27] John Kimionis, Aggelos Bletsas, and John N Sahaalos. Bistatic backscatter radio for tag read-range extension. In *2012 IEEE International Conference on RFID-Technologies and Applications (RFID-TA)*, pages 356–361. IEEE, 2012.
- [28] Songfan Li, Chong Zhang, Yihang Song, Hui Zheng, Lu Liu, Li Lu, and Mo Li. Internet-of-microchips: Direct radio-to-bus communication with spi backscatter. In *The 26th Annual International Conference on Mobile Computing and Networking, MobiCom '20*, London, United Kingdom, 2020. Association for Computing Machinery.
- [29] Yan Li, Zicheng Chi, Xin Liu, and Ting Zhu. Passive-zigbee: Enabling zigbee communication in iot networks with 1000x+ less power consumption. In *Proceedings of the 16th ACM Conference on Embedded Networked Sensor Systems, SenSys '18*, pages 159–171, New York, NY, USA, 2018. Association for Computing Machinery.
- [30] Zhuqi Li, Yaxiong Xie, Longfei Shangguan, Rotman Ivan Zelaya, Jeremy Gummesson, Wenjun Hu, and Kyle Jamieson. Towards programming the radio environment with large arrays of inexpensive antennas. In *16th USENIX Symposium on Networked Systems Design and Implementation (NSDI 19)*, pages 285–300, Boston, MA, February 2019. USENIX Association.
- [31] Vincent Liu, Aaron Parks, Vamsi Talla, Shyamnath Gollakota, David Wetherall, and Joshua R. Smith. Ambient backscatter: Wireless communication out of thin air. In *Proceedings of the ACM SIGCOMM 2013 Conference on SIGCOMM, SIGCOMM '13*, pages 39–50, New York, NY, USA, 2013. Association for Computing Machinery.
- [32] Vincent Liu, Vamsi Talla, and Shyamnath Gollakota. Enabling instantaneous feedback with full-duplex backscatter. In *Proceedings of the 20th Annual International Conference on Mobile Computing and Networking, MobiCom '14*, pages 67–78, New York, NY, USA, 2014. ACM.
- [33] Xin Liu, Zicheng Chi, Wei Wang, Yao Yao, and Ting Zhu. Vmscatter: A versatile mimo backscatter. In *17th USENIX Symposium on Networked Systems Design and Implementation (NSDI '20)*, pages 895–909, 2020.
- [34] Tao Long and Naresh R Shanbhag. Low-power cdma multiuser receiver architectures. In *1999 IEEE Workshop on Signal Processing Systems. SiPS 99. Design and Implementation (Cat. No. 99TH8461)*, pages 493–502. IEEE, 1999.
- [35] Yunfei Ma, Xiaonan Hui, and Edwin C. Kan. 3d real-time indoor localization via broadband nonlinear backscatter in passive devices with centimeter precision. In *Proceedings of the 22nd Annual International Conference on Mobile Computing and Networking, MobiCom '16*, pages 216–229, New York, NY, USA, 2016. Association for Computing Machinery.
- [36] AC McCormick, PM Grant, JS Thompson, T Arslan, and AT Erdogan. Low power receiver architectures for multi-carrier cdma. *IEE Proceedings-Circuits, Devices and Systems*, 149(4):227–233, 2002.

- [37] L.B. Milstein. Interference rejection techniques in spread spectrum communications. *Proceedings of the IEEE*, 76(6):657–671, 1988.
- [38] Carlo Mutti and Christian Floerkemeier. Cdma-based rfid systems in dense scenarios: Concepts and challenges. In *2008 IEEE International Conference on RFID*, pages 215–222. IEEE, 2008.
- [39] Saman Naderiparizi, Mehrdad Hesar, Vamsi Talla, Shyamnath Gollakota, and Joshua R. Smith. Towards battery-free hd video streaming. In *Proceedings of the 15th USENIX Conference on Networked Systems Design and Implementation*, NSDI’18, pages 233–247, USA, 2018. USENIX Association.
- [40] Rajalakshmi Nandakumar, Vikram Iyer, and Shyamnath Gollakota. 3d localization for sub-centimeter sized devices. In *Proceedings of the 16th ACM Conference on Embedded Networked Sensor Systems*, SenSys ’18, pages 108–119, New York, NY, USA, 2018. Association for Computing Machinery.
- [41] Aaron N. Parks, Angli Liu, Shyamnath Gollakota, and Joshua R. Smith. Turbocharging ambient backscatter communication. In *Proceedings of the 2014 ACM Conference on SIGCOMM*, SIGCOMM ’14, pages 619–630, New York, NY, USA, 2014. Association for Computing Machinery.
- [42] Marco Pausini and Gerard J. M. Janssen. Narrowband interference suppression in transmitted reference uwb receivers using sub-band notch filters. In *2006 14th European Signal Processing Conference*, pages 1–5, 2006.
- [43] Yao Peng, Longfei Shangguan, Yue Hu, Yujie Qian, Xi-anhang Lin, Xiaojiang Chen, Dingyi Fang, and Kyle Jamieson. Flora: A passive long-range data network from ambient lora transmissions. In *Proceedings of the 2018 Conference of the ACM Special Interest Group on Data Communication*, SIGCOMM ’18, pages 147–160, New York, NY, USA, 2018. Association for Computing Machinery.
- [44] Carlos Pérez-Penichet, Frederik Hermans, Ambuj Varshney, and Thiemo Voigt. Augmenting iot networks with backscatter-enabled passive sensor tags. In *Proceedings of the 3rd Workshop on Hot Topics in Wireless*, pages 23–27. ACM, 2016.
- [45] Vaishnavi Ranganathan, Sidhant Gupta, Jonathan Lester, Joshua R. Smith, and Desney Tan. Rf bandaid: A fully-analog and passive wireless interface for wearable sensors. *Proc. ACM Interact. Mob. Wearable Ubiquitous Technol.*, 2(2), July 2018.
- [46] Mohammad Rostami, Jeremy Gummeson, Ali Kiaghadi, and Deepak Ganesan. Polymorphic radios: A new design paradigm for ultra-low power communication. In *Proceedings of the 2018 Conference of the ACM Special Interest Group on Data Communication*, SIGCOMM ’18, pages 446–460, New York, NY, USA, 2018. Association for Computing Machinery.
- [47] Mohammad Rostami, Karthik Sundaresan, Eugene Chai, Sampath Rangarajan, and Deepak Ganesan. Redefining passive in backscattering with commodity devices. In *Proceedings of the 26th Annual International Conference on Mobile Computing and Networking*, MobiCom’20, New York, NY, USA, 2020. Association for Computing Machinery.
- [48] Mastrooreh Salajegheh, Shane S Clark, Benjamin Ransford, Kevin Fu, and Ari Juels. Cccp: Secure remote storage for computational rfids. In *USENIX Security Symposium*, pages 215–230, 2009.
- [49] Vamsi Talla, Mehrdad Hesar, Bryce Kellogg, Ali Najafi, Joshua R. Smith, and Shyamnath Gollakota. Lora backscatter: Enabling the vision of ubiquitous connectivity. *Proc. ACM Interact. Mob. Wearable Ubiquitous Technol.*, 1(3), September 2017.
- [50] Vamsi Talla, Joshua Smith, and Shyamnath Gollakota. Advances and open problems in backscatter networking. *GetMobile: Mobile Comp. and Comm.*, 24(4):32–38, March 2021.
- [51] Stewart Thomas and Matthew S Reynolds. Qam backscatter for passive uhf rfid tags. In *2010 IEEE International Conference on RFID (IEEE RFID 2010)*, pages 210–214. IEEE, 2010.
- [52] Stewart J Thomas and Matthew S Reynolds. A 96 mbit/sec, 15.5 pj/bit 16-qam modulator for uhf backscatter communication. In *2012 IEEE International Conference on RFID (RFID)*, pages 185–190. IEEE, 2012.
- [53] Ambuj Varshney, Oliver Harms, Carlos Pérez-Penichet, Christian Rohner, Frederik Hermans, and Thiemo Voigt. Lorea: A backscatter architecture that achieves a long communication range. In *Proceedings of the 15th ACM Conference on Embedded Network Sensor Systems*, pages 1–14, 2017.
- [54] Ambuj Varshney, Carlos Pérez Penichet, Christian Rohner, and Thiemo Voigt. Towards wide-area backscatter networks. In *Proceedings of the 4th ACM Workshop on Hot Topics in Wireless*, pages 49–53, 2017.
- [55] Ambuj Varshney, Andreas Soleiman, and Thiemo Voigt. Tunnelscatter: Low power communication for sensor

- tags using tunnel diodes. In *The 25th Annual International Conference on Mobile Computing and Networking*, MobiCom '19, New York, NY, USA, 2019. Association for Computing Machinery.
- [56] Georgios Vougioukas, Spyridon-Nektarios Daskalakis, and Aggelos Bletsas. Could battery-less scatter radio tags achieve 270-meter range? In *2016 IEEE Wireless Power Transfer Conference (WPTC)*, pages 1–3. IEEE, 2016.
- [57] Anran Wang, Vikram Iyer, Vamsi Talla, Joshua R. Smith, and Shyamnath Gollakota. Fm backscatter: Enabling connected cities and smart fabrics. In *Proceedings of the 14th USENIX Conference on Networked Systems Design and Implementation*, NSDI'17, pages 243–258, USA, 2017. USENIX Association.
- [58] Jingxian Wang, Junbo Zhang, Rajarshi Saha, Haojian Jin, and Swarun Kumar. Pushing the range limits of commercial passive rfids. In *16th USENIX Symposium on Networked Systems Design and Implementation (NSDI 19)*, pages 301–316, Boston, MA, February 2019. USENIX Association.
- [59] Jue Wang, Haitham Hassanieh, Dina Katabi, and Piotr Indyk. Efficient and reliable low-power backscatter networks. In *Proceedings of the ACM SIGCOMM 2012 Conference on Applications, Technologies, Architectures, and Protocols for Computer Communication*, SIGCOMM '12, pages 61–72, New York, NY, USA, 2012. Association for Computing Machinery.
- [60] Po-Han Peter Wang, Chi Zhang, Hongsen Yang, Manideep Dunna, Dinesh Bharadia, and Patrick P. Mercier. A low-power backscatter modulation system communicating across tens of meters with standards-compliant wi-fi transceivers. *IEEE Journal of Solid-State Circuits*, 55(11):2959–2969, 2020.
- [61] Die Wu, Muhammad Jawad Hussain, Songfan Li, and Li Lu. R2: Over-the-air reprogramming on computational rfids. In *2016 IEEE International Conference on RFID (RFID)*, pages 1–8, 2016.
- [62] Lih-Chyau Wu, Yen-Ju Chen, Chi-Hsiang Hung, and Wen-Chung Kuo. Zero-collision rfid tags identification based on cdma. In *2009 Fifth International Conference on Information Assurance and Security*, volume 1, pages 513–516. IEEE, 2009.
- [63] Zhengyuan Xu, B.M. Sadler, and Jin Tang. Data detection for uwb transmitted reference systems with interpulse interference. In *Proceedings. (ICASSP '05). IEEE International Conference on Acoustics, Speech, and Signal Processing, 2005.*, volume 3, pages iii/601–iii/604 Vol. 3, 2005.
- [64] Pengyu Zhang, Dinesh Bharadia, Kiran Joshi, and Sachin Katti. Hitchhike: Practical backscatter using commodity wifi. In *Proceedings of the 14th ACM Conference on Embedded Network Sensor Systems CD-ROM*, SenSys '16, pages 259–271, New York, NY, USA, 2016. Association for Computing Machinery.
- [65] Pengyu Zhang and Deepak Ganesan. Enabling bit-by-bit backscatter communication in severe energy harvesting environments. In *Proceedings of the 11th USENIX Conference on Networked Systems Design and Implementation*, NSDI'14, pages 345–357, USA, 2014. USENIX Association.
- [66] Pengyu Zhang, Jeremy Gummesson, and Deepak Ganesan. Blink: A high throughput link layer for backscatter communication. In *Proceedings of the 10th International Conference on Mobile Systems, Applications, and Services*, MobiSys '12, pages 99–112, New York, NY, USA, 2012. ACM.
- [67] Pengyu Zhang, Pan Hu, Vijay Pasikanti, and Deepak Ganesan. Ekhonet: High speed ultra low-power backscatter for next generation sensors. In *Proceedings of the 20th annual international conference on Mobile computing and networking*, pages 557–568. ACM, 2014.
- [68] Renjie Zhao, Fengyuan Zhu, Yuda Feng, Siyuan Peng, Xiaohua Tian, Hui Yu, and Xinbing Wang. Ofdma-enabled wi-fi backscatter. In *The 25th Annual International Conference on Mobile Computing and Networking*, MobiCom '19, pages 20:1–20:15, New York, NY, USA, 2019. ACM.